International Journal of Progressive Sciences and Technologies (IJPSAT)
ISSN: 2509-0119.

https://ijpsat.org/
Vol. 51 No. 1 June 2025, pp. 16-30

The Optimization Of 3D Printed PLA/EPO/Lignin Biocomposite's Tensile Strength Using Three Different Supervised Learning Applications

Amjad Fakhri Kamarulzaman[1], Yakubu Adekunle Alli[1*], Hazleen Anuar[1*], Mayowa Isiolaotan[2], Mohd Romainor Manshor[1], Bolade Onafuye Atinuke[3], Samuel Oluwadadepo Oni[4], Nwankwo Uche Dickson[5], Caleb Joel Nwaogwugwu[6], Alfred Yeboah[7], Akinyemi Michael Iledare[8]

[1]Department of Manufacturing and Materials Engineering, Kulliyyah of Engineering, International Islamic University Malaysia, Jalan Gombak, 53100 Kuala Lumpur, Malaysia.
[2]Department of Information Systems and Analytics, Middle Tennessee State University, Murfreesboro, Tennessee, 37132, USA
[3]Department of Healthcare Informatics, Middle Tennessee State University, Murfreesboro, Tennessee, 37132, USA
[4]Department of Physics, Georgia Southern University, Statesboro, 30458, USA
[5]Department of Chemistry, Sam Houston State University, Huntsville Texas, 77340, USA
[6]Department of Biochemistry Abia State University, Abia State, Abia, Nigeria
[7]Department of Mining and Minerals, Michigan Technological University, Houghton, 49931
[8]Business Analytical and Insight, University of Wisconsin, 500 Lincoln Dr, Madison, WI 53706, USA
Corresponding authors: Yakubu Adekunle Alli. E-mail: alliyakubu016@gmail.com (Y.A. Alli), Hazleen Anuar. E-mail: hazleen@iium.edu.my (H. Anuar)

Abstract: Developing a sustainable and biodegradable biocomposite for 3D printing necessitates iterative experimentation to achieve the desired composition and properties. Combining polylactic acid (PLA), epoxidized palm oil (EPO), and lignin offers a promising formulation for a 3D biocomposite filament with diverse potential applications. To optimize its performance specifically for 3D printing applications, the use of machine learning techniques can expedite the process of property optimization. Employing three distinct machine learning models, namely random forest (RF), support vector regression (SVR), and artificial neural network (ANN), facilitates a comparative analysis to determine the most effective approach for predicting the tensile strength values across different biocomposite compositions. Through model training and evaluation, the comparison reveals that both RF and SVR demonstrate superior accuracy compared to ANN. Notably, RF exhibits exceptional consistency, boasting an average R2 score of 0.9777 and an average mean squared error of 1.5475. SVR follows closely with an average R2 score of 0.9777 and an average mean squared error of 7.7751, while ANN lags behind with an average R2 score of 0.6551 and an average mean squared error of 117.5218. Assessing the performance of these machine learning models underscores their potential applicability in enhancing the production of biocomposite filaments for 3D printing, thereby facilitating the refinement of biocomposite properties.

Keywords: Machine learning, ANN, SVR, RF, 3D printing

International Journal of Progressive Sciences and Technologies (IJPSAT)
ISSN: 2509-0119.

https://ijpsat.org/
Vol. 51 No. 1 June 2025, pp. 16-30

1.0 Introduction

In recent years, people across various sectors, be it consumers or manufacturers, have extensively embraced 3D printing [1]. Manufacturers employ this technology to create items with intricate dimensions and geometries. At its core, 3D printing relies on a layer-by-layer deposition process, wherein a three-dimensional object is built based on a computer-aided design (CAD) model or a 3D model [2]. However, with the integration of CAD software and innovative materials, the progress of 3D printing can reach an entirely new echelon, enabling products to adapt to diverse functionalities and uses. This technology has progressed to a point where users can independently create their designs and translate them into tangible products [3]. This technological breakthrough enables the straightforward fabrication of 3D models characterized by intricate geometries and complex structures, consequently finding diverse applications in industries such as soft robotics [4] and biomedical devices [5,6].

In recent years, there are some researches that focusing on the production of bio-composite filament to improve the biodegradability of the 3D printing filament while improving its properties [7–10]. A group of researchers has created polylactic acid (PLA) reinforced with alkaline lignin biocomposite to improve the sustainability of the material however the mechanical properties of the filament seem to be degrading since it become brittle [11]. Anuar et. al. has discussed the properties of soda lignin/PLA/EPO biocomposite compared to a regular PLA filament. It shows that the mechanical properties of the biocomposite has increased in its performance which indicate the relevance of the biocomposite [12]. PLA thermoplastic filament has shown significant potential and has been widely used in 3D printing applications [13]. It contains a few properties that contributing the renewability, biocompatibility and biodegradability of a material [14]. Incorporating fillers in PLA composites, such as lignin, help to reinforce the properties of the polymer according to Tanase et. al. The study found that the ductility of PLA biocomposites improved with the addition of reduced lignin concentration. However, for acetylated or unmodified lignin, the flexibility of the biocomposites decreased when the lignin loading was above 10 wt% [15]. The addition of plasticizer helps to counter the brittleness of the biocomposite as demonstrated by Awale et. al. [16].

Machine learning defined as computer algorithms endowed with the capacity for autonomous learning and data interpretation. Relying predominantly on these algorithms, human intervention for result determination is largely unnecessary [17]. The core objective of machine learning is to discern data patterns and construct models based on input and output data, thereby fulfilling its purpose [18–20]. The method that has been applied for this study is supervised learning where the algorithm undergoes training using available dataset examples to enable classification and prediction of system outputs [21]. The system model's refinement involves adjusting parameter weights until the desired results are attained. This process is necessary to prevent issues of underfitting or overfitting within the system model.

In the new era, machine learning has become a big factor in optimizing the properties of biocomposite. For instance, machine learning model can be utilized for predicting the compressive strength and thermal conductivity of a biocomposite. Xu et. al. has applied three different machine learning methods, which are deep neural network (DNN), gene expression programming (GEP) and optimizable Gaussian process regressor (OGPR) [22]. All of them has shown consistency in the compressive strength and thermal conductivity of the biocomposite which make the machine learning model more reliable. Other studies show that machine learning also can be used to classify the feature of acoustic emission in biocomposite in order to evaluate the material behavior under challenging low temperature environments [23].

Given the relatively limited utilization of machine learning in biocomposite applications, it becomes imperative to explore its potential for enhancing the integration of biocomposites in 3D printing, particularly in the optimization of their mechanical properties. This research delved into the application of three distinct machine learning algorithms—namely, artificial intelligence neural network (ANN), support vector regression (SVR), and random forest (RF)—to fine-tune the tensile strength of the PLA/EPO/Lignin filament. Through the evaluation of the tensile strength using the ANN, SVR, and RF models, the study effectively demonstrated the predictive capabilities of these models across various biocomposite compositions. The novelty of this research lies in the combination of unique biocomposite materials, the specific focus on optimizing tensile strength through 3D printing, and the application of various supervised learning techniques to achieve this optimization. The integration of

machine learning into the realm of material science enhances the efficiency and precision of the optimization process, contributing to the overall advancement of both materials' science and machine learning applications

2.0 Material and Methods

2.1 Material preparation

The oil palm empty fruit bunch (OPEFB) fibers underwent preliminary processing to eliminate impurities, collected from Tennamaram Palm Oil Mill, Batang Berjuntai, Selangor. Through manual sorting, sediment and kernel shells were separated from the fibers. After drying in a high-speed air convection oven at 60 °C for a span of 24 hours, the cleaned fibers were crushed and ground, yielding finer fibers. Subsequently, a sieve shaker was employed to segregate the larger OPEFB fibers.

The separation of lignin from OPEFB fibers was executed using a chemical process involving alkaline extraction to produce alkaline lignin. Alkaline lignin powder was combined with EPO and PLA pellets in a manual mixing process at different weight fractions (phr) between PLA, EPO and lignin powder was presented in Table 1. EPO with density of 0.886 g/mL and oxirane oxygen content of 2.84 was obtained from Budi Oil Enterprise Sdn Bhd, Telok Gong, Port Klang, Selangor, Malaysia, while PLA grade 2003D in the form of pellets was supplied by NatureWorks Co. Ltd. Using the FILABOT EX6 Extruder, the mixtures were extruded consecutively at temperatures of 180 °C, 190 °C, 180 °C, and 50 °C. The resulting filaments were then placed in a desiccator with 0% relative humidity for subsequent characterization.

Thermogravimetric analysis (TGA) of bio-composite filaments were performed using a Perkin Elmer thermogravimetric analyzer (TGA4000). The samples were conducted with temperature ranged from 30 °C to 600 °C with a heating rate of 10 °C/min under nitrogen atmosphere to examine the thermal degradation behavior. Approximately 5 mg of samples were prepared for the thermogravimetric analysis. Differential scanning calorimetry (DSC) was carried out using a Mettler Toledo DSC821e to obtain the glass transition (T_g) temperature and on-set (T_o) temperature.

Table 1: Composition of PLA/lignin/EPO bio-composite

Material Designation	PLA (phr)	Lignin (phr)	EPO (phr)
PLA	100	-	-
PLAL1	100	1	-
PLAE1	100	1	5

2.2. Data collection

The PLA/lignin bio-composite filaments underwent assessment using a universal testing machine (UTM) equipped with a 5 kN load cell, operating at a crosshead speed of 2.5 mm/min. The tensile strength, tensile modulus, and tensile strain of the composites were evaluated under room temperature conditions (25 ± 2°C) and at a relative humidity of 50 ± 5%. To determine these properties, filament samples were prepared and tested for each composition, employing a gauge length of 25 mm. Furthermore, the tensile test on the 3D-printed PLA-lignin biocomposites adhered to the guidelines of ASTM D638-14, Type I. To achieve this, the tensile dumbbell specimens were produced for different composition, utilizing a similar testing machine setup. The data that has been collected for optimizing the tensile strength optimization are stress and strain for every time the tensile testing is conducted. The data that will be utilized in for the machine learning model was from the initial part of the tensile testing until it achieves its peak stress as shown in **Figure 1**.

International Journal of Progressive Sciences and Technologies (IJPSAT)
ISSN: 2509-0119.

https://ijpsat.org/
Vol. 51 No. 1 June 2025, pp. 16-30

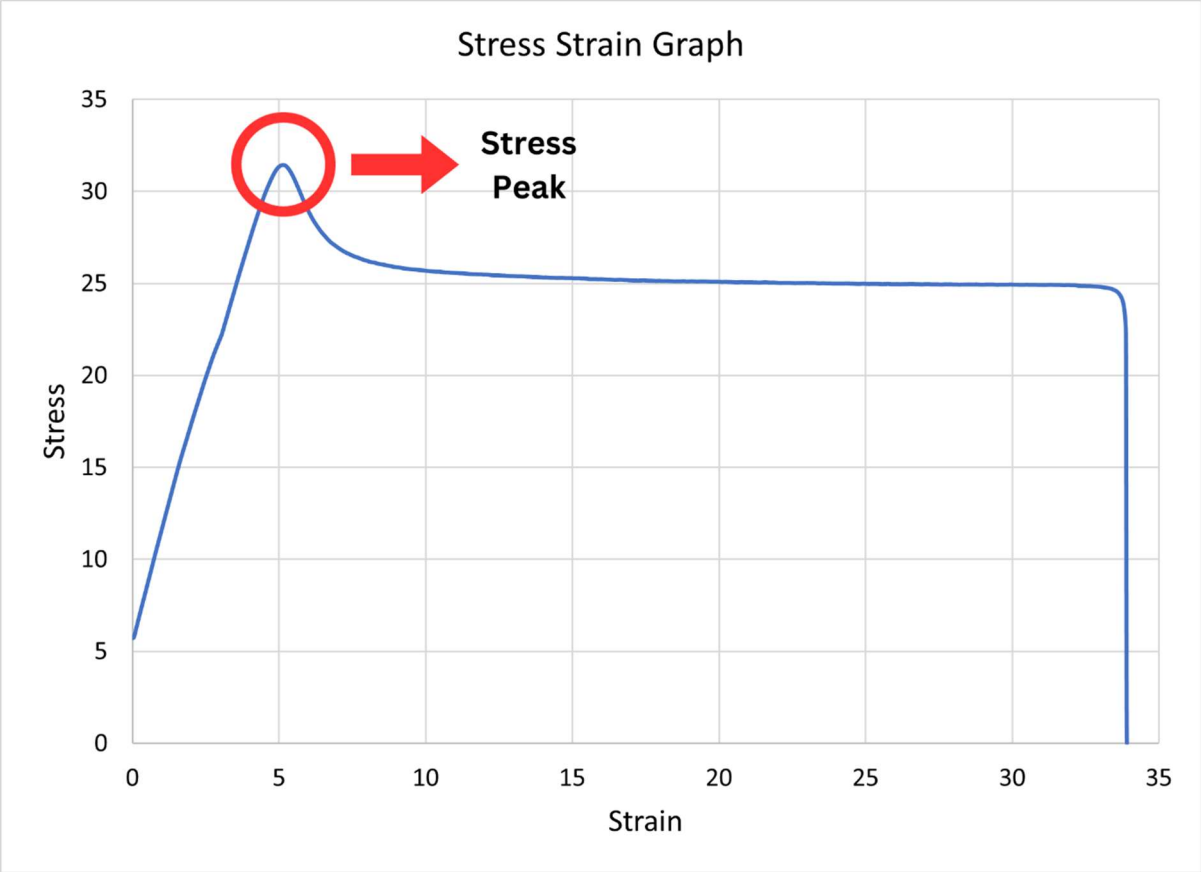

Figure 1: Stress Strain Peak

2.3. Machine learning methods

In this paper, three different machine learning methods that has been utilized to predict the tensile strength of PLA/EPO/lignin biocomposite for different composition. All the machine learning model is created using Python programming using the Anaconda environment with Keras library as the main body for ANN development while Scikit-learn library as the main body for RF and SVR, while analysing the error for all machine learning model. RF model is an ensemble tree that is created from a previous set of training. The best split is determined from the input features or random subset of size maximum features. RF can reduce the variance of the results by combining diverse trees. The model of RF for regression approaches is formed from growing trees that depends on a random vector in which the tree predictor, *h(x,k)* handles the numerical values rather than class labels. The RF predictor is formed by taking the average over *k* of the trees. Equation 1 shows the general equation for RF model.

$$\hat{f} = \frac{1}{B}\sum_{b=1}^{B} f_b(x') \quad (1)$$

SVR, a component of the support vector machine (SVM) method, is utilized for generating continuous outputs from a finite set. It introduces the concept of ε-insensitive regions or hyperplanes. Rather than minimizing the error between actual and predicted values, SVR attempts to fit a best fit line within the hyperplane and its boundary values, known as threshold values. Due to its increasing quadratic complexity with a growing number of samples, SVR is applicable for small-scale datasets. The SVR function's approximation is represented as shown in Equation 2, while for multidimensional data, the mathematical representation of SVR can be referenced as in Equation 3.

$$f(x) = < w, x > + b = \sum_{j=1}^{M} w_j x_j + b, y, b \in \mathbb{R}, x, w \in \mathbb{R}^M \quad (2)$$

International Journal of Progressive Sciences and Technologies (IJPSAT)
ISSN: 2509-0119.

https://ijpsat.org/
Vol. 51 No. 1 June 2025, pp. 16-30

$$f(x) = \begin{bmatrix} w \\ b \end{bmatrix}^T \begin{bmatrix} x \\ 1 \end{bmatrix} = w^T x + b \quad x, w \in \mathbb{R}^{M+1} \tag{3}$$

Furthermore, ANN relatively a relationship between input and output data which included with training process to get the optimal accuracy and consistent model. The ability to self-learning self-adaptability from previous generation made ANN a better method to get a better estimation than usual statistical analysis method. The architecture for ANN consists of 3 main parts, which are input layer, output layer and hidden layer as shown in **Figure 2**. Each layer will be included with its own weights, activation function and biases which all of them have its own functionality to produce the optimal output for the model. Weight in ANN model can determine which neuron has the highest impact to the output compared to other neurons while biases act as an offset for the output to gain the optimal fit from the given input data. The function of activation function is to filter which data that will be used in the next layer to eliminate some losses during the training. The mathematical model for ANN can be expressed as Equation 4 which consists of weights, biases, and activation function.

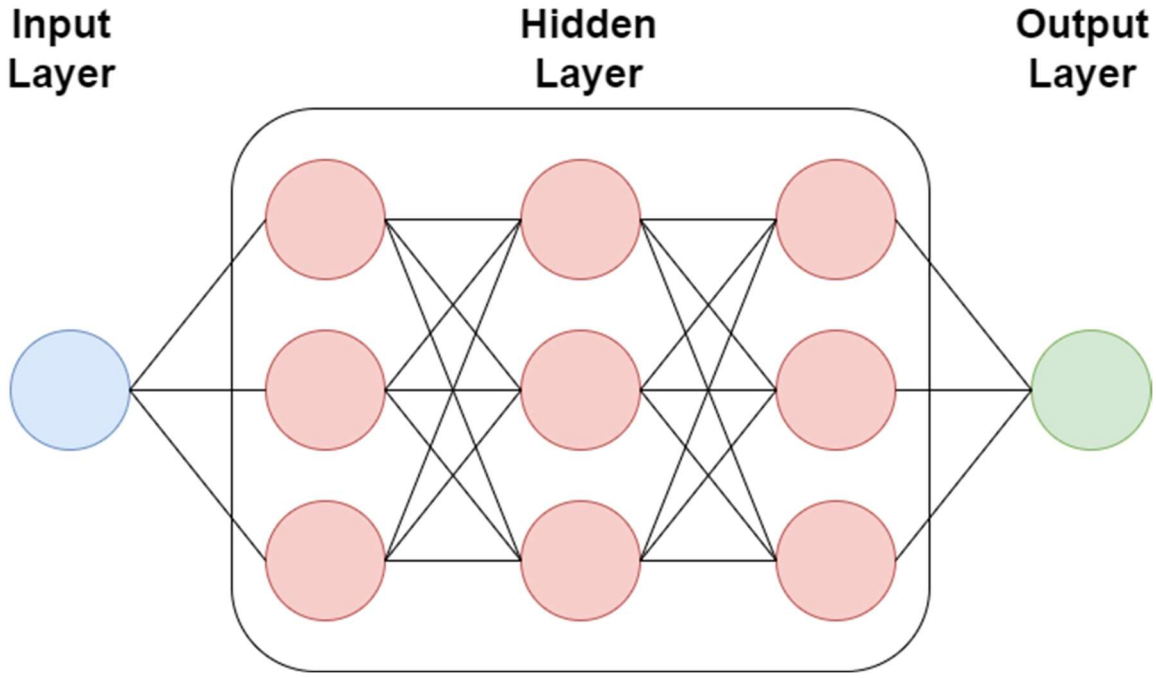

Figure 2: ANN architecture

$$\sum_{i=k}^{m} w_i x_i + bias = w_1 x_1 + w_2 x_2 + \cdots + w_k x_k + bias \tag{4}$$

2.4. Error evaluation

Three methods of error evaluation are utilized to measure and compare the performance of each trained machine learning model. These methods include the coefficient of determination, also known as the R2 score, as well as the mean squared error (MSE) and the root mean squared error (RMSE). The R2 score serves as a statistical metric for assessing the disparity between the model's predicted values and the actual experimental values within the dataset. It can be expressed as shown in **Equation 5**. The R2 score ranges from 0 to 1, with higher values indicating greater accuracy of the results.

$$R^2 = 1 - \frac{\sum(Y_i - Y_p)^2}{\sum(Y_i - Y_m)^2} \tag{5}$$

MSE, on the other hand, is a statistical metric that quantifies the standard deviation of the prediction error. Computed from the Euclidean distance, MSE always yields a positive loss value, with the error diminishing as the loss value approaches zero, as depicted in **Equation 6**. Numerous variations of MSE, including RMSE, share a similar purpose, with RMSE serving as the

square root of MSE. RMSE is a scaled representation of MSE, facilitating the visual depiction of errors in graphical figures, as shown in **Equation 7**.

$$MSE = \frac{1}{n}\sum_{i=1}^{n}(Y_i - \hat{Y}_i)^2 \quad (6)$$

$$RMSE = \sqrt{\frac{1}{n}\sum_{i=1}^{n}(Y_i - \hat{Y}_i)^2} \quad (7)$$

3.0. Results and Discussion

3.1. Thermogravimetric Analysis (TGA) and Differential Scanning Calorimetry (DSC)

TGA analysis of the PLA/lignin/EPO bio-composites were conducted to observe the changes in thermal characteristics of PLA upon addition of lignin as filler and EPO as plasticizer. Observation on the thermal behaviour of the bio-composite, mainly on the thermal degradation is necessary in this study due to exertion of the thermal processing such as extrusion and 3D printing that require material to be thermally stable. Hence, the glass transition temperature (T_g) curves of PLA/lignin/EPO were presented in **Figure 3a.** The T_g of these printed bio-composites exhibited quite similar thermal degradation behavior, where the on-set temperature (T_o) occurs at around 338 ºC, 344 ºC and 340 ºC for PLA, PLAE1 and PLAL1 respectively. The result showed that upon undergone another melting and cooling process of 3D printing, T_o of bio-composites with addition of lignin (PLAE1 and PLAL1) were higher compared to pure PLA. This has proven that addition of lignin had produce better thermal stability, lowering the rate of degradation during the 3D printing process. This behaviour will contribute to better mechanical properties of 3D printed bio-composites, as compared to pure PLA.

Differential scanning calorimetry analysis was also conducted to observe the thermal features of the PLA/lignin bio-composites, mainly the T_g and melting temperature (T_m).These thermal properties were shown in **Figure 3b.** The T_g, and melting temperature (T_m) pure filament PLA bio-composite were 61 ºC, and 152 ºC respectively. In comparison, the T_g of PLA/lignin bio-composites with addition of lignin and EPO were reduced, with 59 ºC and 57 ºC for PLAL1 and PLAE1 respectively. This condition may be attributed to the molecular factors such as intermolecular hydrogen bond and rigid phenyl groups of lignin component. The T_m of PLAL1 and PLAE1 was found lower compared to pure PLA, around 150 ºC, in which about 2 ºC decrement. As explained previously, PLA required more time and temperature for reorganization of crystal can occur. Other than that, both PLAL1 and PLAE1 had two distinguishable T_m peaks at around 150 ºC and 155 ºC, resulted from the melting-recrystallization process occurred in the bio-composite.

International Journal of Progressive Sciences and Technologies (IJPSAT)
ISSN: 2509-0119.

https://ijpsat.org/
Vol. 51 No. 1 June 2025, pp. 16-30

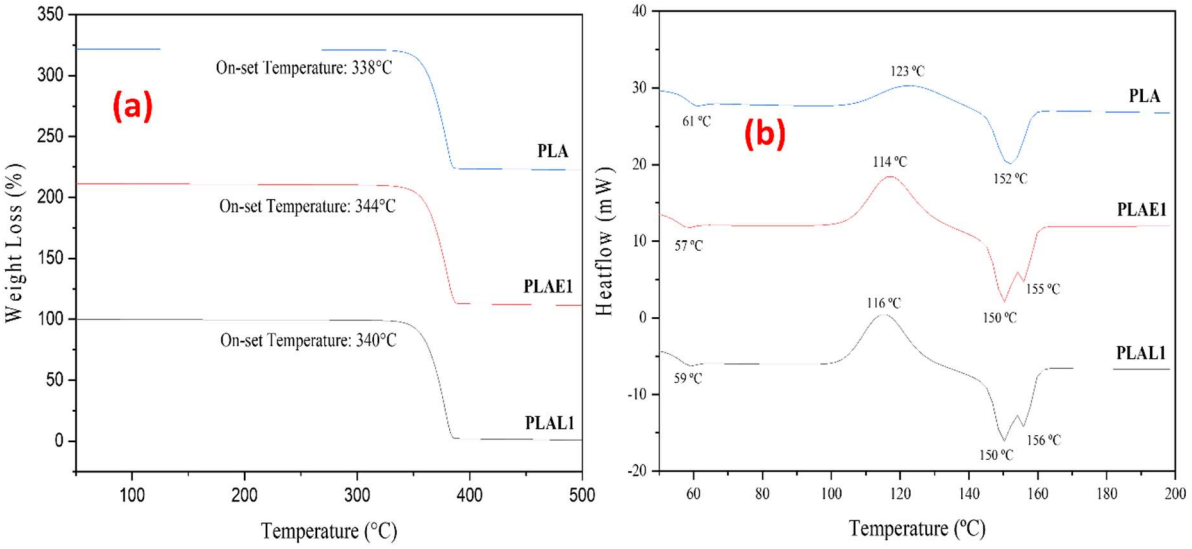

Figure 3: Thermal properties of PLA/lignin/EPO bio-composites; (a) TG curves, (b) DSC curves

3.2 Predicted results

Table 2 presented below provides a comparison of the actual experimental tensile strength data with the predicted values generated by three distinct machine learning models: RF, SVR, and ANN. These machine learning models were configured in a simplified manner to accommodate the characteristics of a small dataset, as small datasets typically necessitate straightforward model adjustments for optimization. The configuration details for each model employed in this study are summarized in **Table 3**.

Table 2: Previous research related to this study

Machine Learning Model	Configuration
Random Forest	• Number of estimators: 10 • Random state: 0 • Verbose: 0 • Number of jobs: 1 • Minimum sample split: 2 • Maximum depth: None
Support Vector Regression	• Kernel: rbf • Degree: 3 • Gamma: 1 • Coefficicent: 0.0 • Regularization parameter (C): 1.0 • Epsilon: 1.0
Artificial Neural Network	• Input Layer: 1 • Hidden Layer: 3

	○ First Layer: 30, Activation: ReLU ○ Second Layer: 20, Activation: ReLU ○ Third Layer: 10, Activation: ReLU • Output Layer: 1, Activation: Linear • Optimizer: Adam

Table 3: Machine Learning Model Configuration

Sample	Actual Tensile Strength (MPa)	Predicted Tensile Strength (MPa)		
		RF	SVR	ANN
Sample 1	32.81385	33.166747	32.809856	33.530106
Sample 2	27.17819	27.847955	27.576785	28.12973
Sample 3	31.02034	30.5407695	30.276263	30.96951
Sample 4	32.92646	32.308612	32.163885	33.673714

According to the data presented in **Table 4**, the machine learning models exhibited a relatively precise prediction of the peak stress for the PLA/EPO/Lignin filament. The standard deviation and standard error for each sample were calculated using Equation (8) and Equation (9) to evaluate the deviation of the predicted data. The computed standard deviations for the samples were 0.29746, 0.35103, 0.30828, and 0.59612, while the standard errors were 0.14873, 0.17552, 0.15414, and 0.29806, respectively. Analysis of the standard deviation and error derived from the predicted results indicated a minimal dispersion of the data from the trained models, affirming the reliability and accuracy of the trained models. This type of trend have been reported by Fatriansyah and co-workers in their recent publication [24].

$$\sigma = \sqrt{\frac{1}{N}\sum_{i=1}^{N}(x_i - \mu)^2} \quad (8)$$

$$\sigma_{\bar{x}} = \frac{\sigma}{\sqrt{N}} \quad (9)$$

Table 4: Comparison Between Actual and Predicted Tensile Strength Data

Sample	R^2 Score			MSE		
	RF	SVR	ANN	RF	SVR	ANN
Sample 1	0.99801	0.99824	0.63047	0.178121	0.156202	133.4172
Sample 2	0.95483	0.95532	0.38117	2.794643	27.576785	152.4251
Sample 3	0.96123	0.96026	0.79019	2.931541	2.984236	111.3717
Sample 4	0.99682	0.99680	0.81864	0.2855498	0.286385	72.8730

The RF, SVR, and ANN models were initially trained using the raw data spanning from the early stages of tensile testing to the point of reaching peak stress for each respective sample. Subsequently, a line graph was constructed to monitor the trends in training, validation, and prediction data for comparison of the performance of each trained model. As depicted in **Figures 4 (a-d)** and **5 (a-d)**, the RF and SVR models excelled in closely approximating the experimental value trends. In contrast, the ANN model

International Journal of Progressive Sciences and Technologies (IJPSAT)
ISSN: 2509-0119.

https://ijpsat.org/
Vol. 51 No. 1 June 2025, pp. 16-30

exhibited inaccuracies in its predictions, resulting in a consistent, linear trend that persisted until reaching the stress peak, as illustrated in **Figure 6 (a-d).** This suggests that the simpler architecture of the ANN model was inadequate for accurately modeling the nonlinearity of the data and capturing a more precise trend

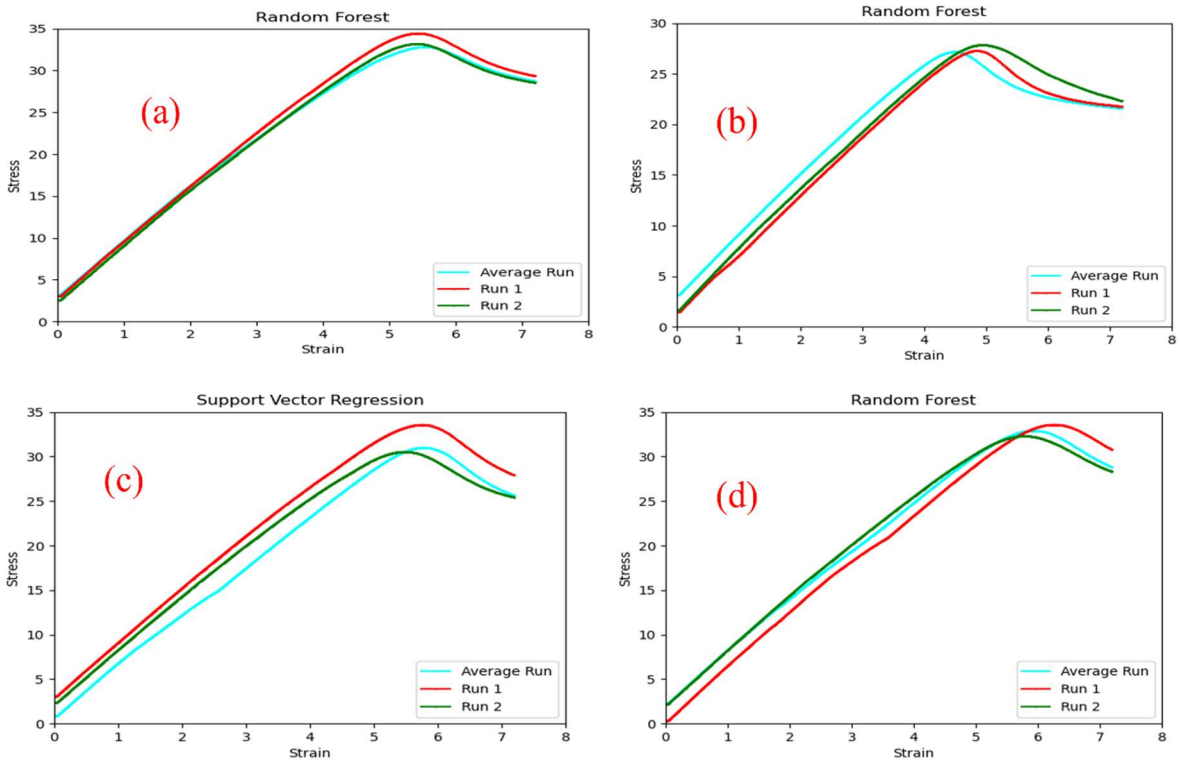

Figure 4: RF Prediction of (a) Sample 1 (b) Sample 2 (c) Sample 3 (d) Sample 4

International Journal of Progressive Sciences and Technologies (IJPSAT)
ISSN: 2509-0119.

https://ijpsat.org/
Vol. 51 No. 1 June 2025, pp. 16-30

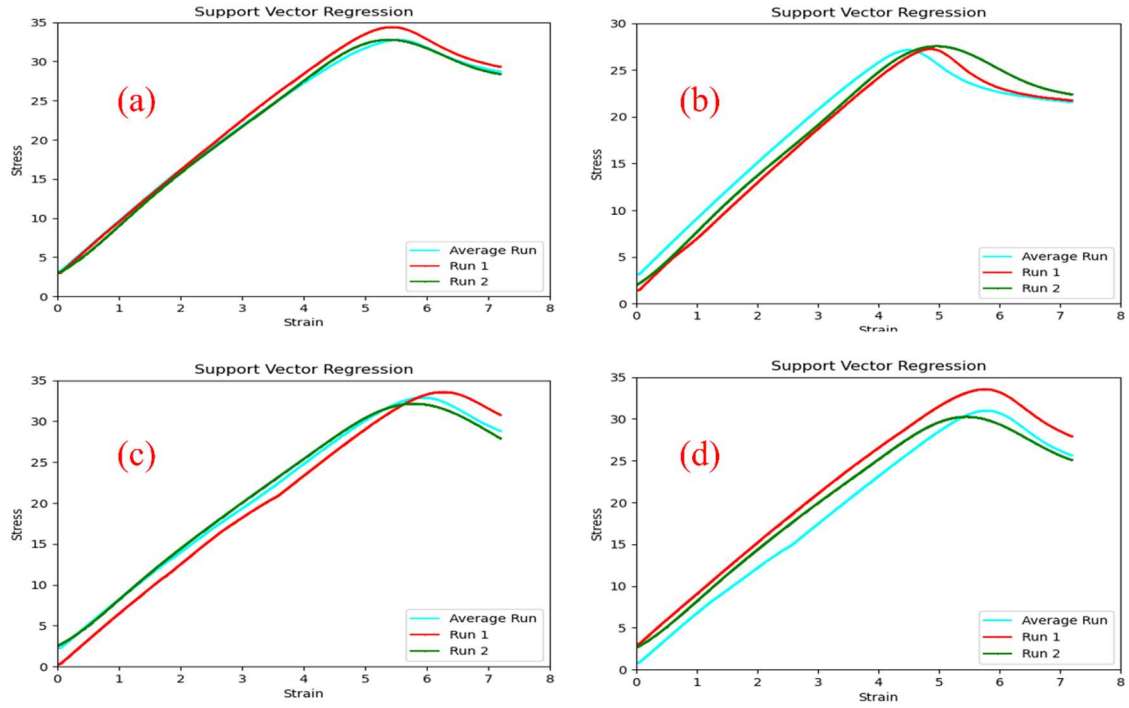

Figure 5: SVR Prediction of (a) Sample 1 (b) Sample 2 (c) Sample 3 (d) Sample 4

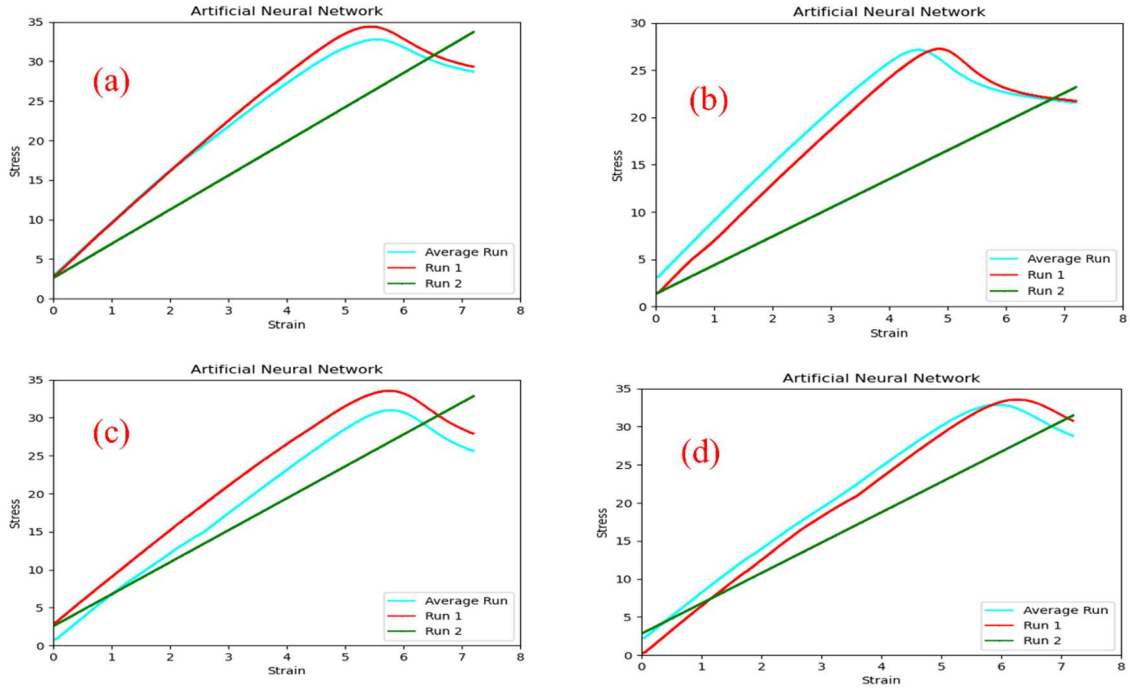

Figure 6: ANN Prediction of (a) Sample 1 (b) Sample 2 (c) Sample 3 (d) Sample 4

International Journal of Progressive Sciences and Technologies (IJPSAT)
ISSN: 2509-0119.

https://ijpsat.org/
Vol. 51 No. 1 June 2025, pp. 16-30

3.2. Performance Analysis

To demonstrate the precision and consistency of both the actual experimental data and the predicted data, a scatter plot was generated, as depicted in **Figure 7 a-c**. The graph's best fit line demonstrated the proximity of the validation data's predictions to each trained model. Both the RF and SVR models exhibited strong predictive capabilities, as the predicted data for various samples were evenly distributed around the best fit line. Conversely, the ANN model slightly skewed towards the upper side of the best fit line. Given the limited sample size, the dataset could not entirely reflect the accuracy of the predicted data in comparison to the actual experimental data.

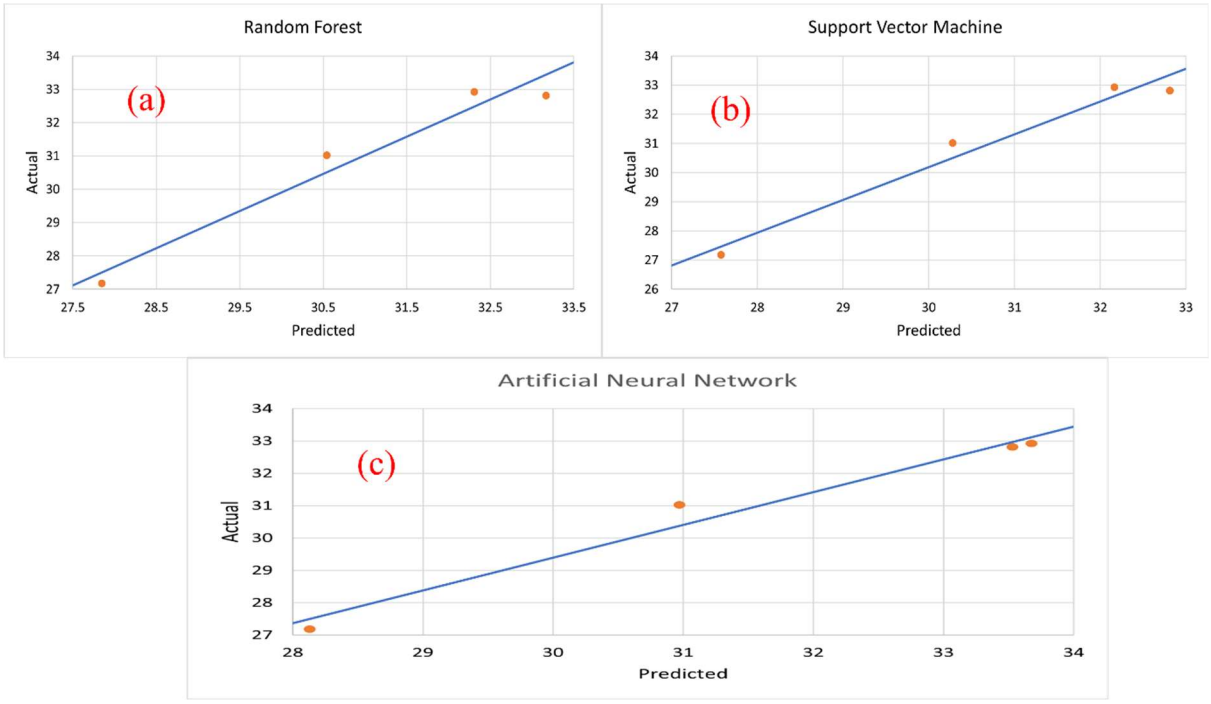

Figure 7: Actual vs Prediction Graph of (a) RF model (b) SVR model (c) ANN model

The performance assessment of the trained RF, SVR, and ANN models was conducted using the R2 score, MSE, and RMSE. The R2 score, depicted in **Figure 8(a)** via the best fit line, served as an indicator of the accuracy level of the prediction data in relation to the validation data. Both the RF and SVR models displayed notably high R2 scores, signifying their accuracy and consistency. For the ANN model, the R2 score for the tensile strength of samples 3 and 4 exhibited a favorable level of accuracy and consistency, while samples 1 and 2 demonstrated intermediate and low levels of accuracy and consistency, respectively, in predicting the output. These findings suggest that the ANN model requires further adjustments or modifications to enhance its output prediction. **Figure 8** illustrates the distinct performance differences among the RF, SVR, and ANN models when comparing the prediction data with the validation data.

International Journal of Progressive Sciences and Technologies (IJPSAT)
ISSN: 2509-0119.

https://ijpsat.org/
Vol. 51 No. 1 June 2025, pp. 16-30

Figure 8: (a) R2 Score (b) RMSE comparison for RF, SVR and ANN model

Furthermore, the MSE serves the purpose of offering an assessment of the overall error in the trained models. Notably, the RF models exhibited the best overall MSE performance compared to the SVR and ANN models, as they consistently maintained the MSE value below 3. In most cases, the SVR models demonstrated low MSE values, which were comparable to the performance of the RF model. However, the SVR model for sample 2 displayed a slightly higher MSE value, indicating a minor inconsistency in the model. On the other hand, the ANN models exhibited the least favorable MSE values due to their inaccuracies and instability in predicting the tensile strength of each sample. **Figure 8b** presents the RMSE values for each machine learning model across different samples. The choice of RMSE over MSE in **Figure 8b** is attributed to RMSE being a variation of MSE that is easier to visualize and compare across various samples and models in this study.

Comparing the findings of this study with prior research is essential. For instance, a group of researchers previously devised three separate machine learning models to forecast the compressive strength and thermal conductivity of hemp biocomposites. These models encompassed deep neural network (DNN), gene expression programming (GEP), and Gaussian process regressor (GSR) [25]. The researchers successfully developed all machine learning models with high accuracy, even when working with a limited dataset for the experiment. Moreover, Lyngdoh et al. utilized the ANN model to predict the strain-sensing ability for a nano-engineered cementitious composite, employing approximately 3000 collected datasets [26]. The ANN models exhibited a strong correlation between the predictive effectiveness and the comparison of simulation results with experimental outcomes.

Nevertheless, several related studies were referenced, although not directly focused on composite materials, particularly in the context of biocomposite applications, as the concept remains within the realm of interest. For instance, Lin et al. have delved into the performance evaluation of four distinct machine learning models, including linear regression, the Lasso algorithm, K-nearest neighbor (KNN), and gradient boosting [27]. The research highlights the variation in performance among different machine learning models for the specific data collected. Table 5 below summarized the compared results from the recent studies.

In light of this, the current study stands as a promising endeavor in predicting the tensile strength of 3D printing.

Table 5: Error Evaluation Comparison Between RF, SVR and ANN

Material	Characterization	Optimization Method	References
Hemp biocomposite	Compressive strength and thermal conductivity	ANN	[28]
Nano-engineered cementitious composite	Strain-sensing ability	DNN, GEP, GSR	[25]
Fibrous paper material	Failure strain, effective stiffness, and maximal stress of fibre networks under tensile test	Linear regression, Lasso algorithm, KNN and gradient boosting	[29]

4. Conclusions

The analysis compares three models for predicting the tensile strength of a PLA/EPO/Lignin biocomposite filament. Random Forest (RF) outperforms Support Vector Regression (SVR) and Artificial Neural Network (ANN), exhibiting the highest average R2 score of 0.9777 and the lowest average MSE value of 1.5475 across various sample compositions. While SVR shows generally accurate predictions, inconsistencies, particularly with sample 3 data, prompt the need for modifications. The ANN model, while promising, suffers from unreliability and inconsistency due to a relatively small training dataset, suggesting potential improvement with an expanded dataset. To refine optimization, considerations include increasing dataset size during training, exploring alternative regression models like XGBoost and KNN, and tuning specific parameters for SVR and ANN. Additionally, integrating optimization models such as genetic algorithms or particle swarm optimization could enhance prediction accuracy for biocomposite properties.

Acknowledgement

The authors would like to thank Kulliyyah of Engineering, International Islamic University Malaysia (IIUM), and the Asian Office of Aerospace Research and Development (AOARD) grant through collaborative research with Sungkyunkwan University (FA2386-22-1-4041) for the financial support.

Funding

This work was supported by the Asian Office of Aerospace Research and Development (AOARD) (FA2386-22-1-4041).

Conflict of Interest

The author declares no conflict of interest.

References

[1] A. Muzaffar, M.B. Ahamed, K. Deshmukh, T. Kovářík, T. Křenek, S.K.K. Pasha, 3D and 4D printing of pH-responsive and functional polymers and their composites, in: 3D and 4D Printing of Polymer Nanocomposite Materials: Processes, Applications, and Challenges, Elsevier, 2019: pp. 85–117. https://doi.org/10.1016/B978-0-12-816805-9.00004-1.

[2] B. Muñiz Castro, M. Elbadawi, J.J. Ong, T. Pollard, Z. Song, S. Gaisford, G. Pérez, A.W. Basit, P. Cabalar, A. Goyanes, Machine learning predicts 3D printing performance of over 900 drug delivery systems, Journal of Controlled Release 337 (2021) 530–545. https://doi.org/10.1016/j.jconrel.2021.07.046.

[3] G.D. Goh, S.L. Sing, W.Y. Yeong, A review on machine learning in 3D printing: applications, potential, and challenges, Artif Intell Rev 54 (2021) 63–94. https://doi.org/10.1007/s10462-020-09876-9.

[4] A. Zolfagharian, L. Durran, S. Gharaie, B. Rolfe, A. Kaynak, M. Bodaghi, 4D printing soft robots guided by machine learning and finite element models, Sens Actuators A Phys 328 (2021). https://doi.org/10.1016/j.sna.2021.112774.

[5] S. Akbari, Y.-F. Zhang, D. Wang, Q. Ge, 4D Printing and Its Biomedical Applications, in: 3D and 4D Printing in Biomedical Applications, Wiley-VCH Verlag GmbH & Co. KGaA, Weinheim, Germany, 2018: pp. 343–372. https://doi.org/10.1002/9783527813704.ch14.

[6] M. Elbadawi, L.E. McCoubrey, F.K.H. Gavins, J.J. Ong, A. Goyanes, S. Gaisford, A.W. Basit, Disrupting 3D printing of medicines with machine learning, Trends Pharmacol Sci 42 (2021) 745–757. https://doi.org/10.1016/j.tips.2021.06.002.

[7] S. Ponis, E. Aretoulaki, T.N. Maroutas, G. Plakas, K. Dimogiorgi, A systematic literature review on additive manufacturing in the context of circular economy, Sustainability (Switzerland) 13 (2021). https://doi.org/10.3390/su13116007.

[8] Q. Ge, Y. Mao, K. Yu, M.L. Dunn, H. Jerry Qi, Active composites and 4D printing, in: ICCM International Conferences on Composite Materials, 2015.

[9] S. Ulag, C. Kalkandelen, T. Bedir, G. Erdemir, S.E. Kuruca, F. Dumludag, C.B. Ustundag, E. Rayaman, N. Ekren, B. Kilic, O. Gunduz, Fabrication of three-dimensional PCL/BiFeO3 scaffolds for biomedical applications, Materials Science and Engineering: B 261 (2020) 114660. https://doi.org/10.1016/J.MSEB.2020.114660.

[10] Y.O. Kewuyemi, H. Kesa, R. Meijboom, O.A. Alimi, O.A. Adebo, 3D food printing improves color profile and structural properties of the derived novel whole-grain sourdough and malt biscuits, Sci Rep 12 (2022) 1–11.

[11] N.A.A. Rahman, H. Anuar, F. Ali, J. Suhr, Poly(Lactic) Acid Reinforced with Alkaline Lignin Biocomposites Prepared by Thermal Extrusion for Sustainable 3D Printing Process, J Phys Conf Ser 2129 (2021) 1–7. https://doi.org/10.1088/1742-6596/2129/1/012003.

[12] H. Anuar, N.A.A. Rahman, M.R. Manshor, Y.A. Alli, O.A. Alimi, F. Alif, J. Suhr, Novel soda lignin/PLA/EPO biocomposite: A promising and sustainable material for 3D printing filament, Mater Today Commun 35 (2023) 106093. https://doi.org/10.1016/J.MTCOMM.2023.106093.

[13] O.A. Alimi, N. Bingwa, R. Meijboom, Homemade 3-D printed flow reactors for heterogeneous catalysis, Chemical Engineering Research and Design 150 (2019) 116–129.

[14] Z. Liu, Y. Wang, B. Wu, C. Cui, Y. Guo, C. Yan, A critical review of fused deposition modeling 3D printing technology in manufacturing polylactic acid parts, The International Journal of Advanced Manufacturing Technology 102 (2019) 2877–2889. https://doi.org/10.1007/s00170-019-03332-x.

[15] M. Tanase-Opedal, E. Espinosa, A. Rodríguez, G. Chinga-Carrasco, Lignin: A biopolymer from forestry biomass for biocomposites and 3D printing, Materials 12 (2019) 1–15. https://doi.org/10.3390/ma12183006.

[16] R.J. Awale, F.B. Ali, A.S. Azmi, N.I.M. Puad, H. Anuar, A. Hassan, Enhanced flexibility of biodegradable polylactic acid/starch blends using epoxidized palm oil as plasticizer, Polymers (Basel) 10 (2018). https://doi.org/10.3390/polym10090977.

[17] E. Alpaydin, Introduction to Machine Learning, 3rd Editio, The MIT Press, London, 2014.

[18] M. Mohammed, M.B. Khan, E.B.M. Bashie, Machine learning: Algorithms and applications, CRC Press, 2016. https://doi.org/10.1201/9781315371658.

[19] M.A. Mahmood, A.I. Visan, C. Ristoscu, I.N. Mihailescu, Artificial Neural Network Algorithms for 3D Printing, Materials 14 (2020) 163. https://doi.org/10.3390/ma14010163.

[20] E. Alpaydin, Introducing to Machine Learning Third Edition, 3rd Editio, The MIT Press, London, 2014.

[21] M. Alloghani, D. Al-Jumeily, J. Mustafina, A. Hussain, A.J. Aljaaf, A Systematic Review on Supervised and Unsupervised Machine Learning Algorithms for Data Science, in: 2020: pp. 3–21. https://doi.org/10.1007/978-3-030-22475-2_1.

[22] G. Xu, G. Zhou, F. Althoey, H.M. Hadidi, A. Alaskar, A.M. Hassan, F. Farooq, Evaluation of properties of bio-composite with interpretable machine learning approaches: optimization and hyper tuning, Journal of Materials Research and Technology 25 (2023) 1421–1446. https://doi.org/10.1016/j.jmrt.2023.06.007.

[23] T. Kek, P. Potočnik, M. Misson, Z. Bergant, M. Sorgente, E. Govekar, R. Šturm, Characterization of Biocomposites and Glass Fiber Epoxy Composites Based on Acoustic Emission Signals, Deep Feature Extraction, and Machine Learning, Sensors 22 (2022). https://doi.org/10.3390/s22186886.

[24] J.F. Fatriansyah, E. Kustiyah, S.N. Surip, A. Federico, A.F. Pradana, A.S. Handayani, M. Jaafar, D. Dhaneswara, Fine-tuning optimization of poly lactic acid impact strength with variation of plasticizer using simple supervised machine learning methods, Express Polym Lett 17 (2023) 964–973. https://doi.org/10.3144/expresspolymlett.2023.71.

[25] G. Xu, G. Zhou, F. Althoey, H.M. Hadidi, A. Alaskar, A.M. Hassan, F. Farooq, Evaluation of properties of bio-composite with interpretable machine learning approaches: optimization and hyper tuning, Journal of Materials Research and Technology 25 (2023) 1421–1446. https://doi.org/10.1016/j.jmrt.2023.06.007.

[26] G.A. Lyngdoh, S. Das, Integrating multiscale numerical simulations with machine learning to predict the strain sensing efficiency of nano-engineered smart cementitious composites, Mater Des 209 (2021) 109995. https://doi.org/10.1016/j.matdes.2021.109995.

[27] B. Lin, Y. Bai, B.X. Xu, Data-driven microstructure sensitivity study of fibrous paper materials, Mater Des 197 (2021) 109193. https://doi.org/10.1016/j.matdes.2020.109193.

[28] G.A. Lyngdoh, S. Das, Integrating multiscale numerical simulations with machine learning to predict the strain sensing efficiency of nano-engineered smart cementitious composites, Mater Des 209 (2021) 109995. https://doi.org/10.1016/j.matdes.2021.109995.

[29] B. Lin, Y. Bai, B.X. Xu, Data-driven microstructure sensitivity study of fibrous paper materials, Mater Des 197 (2021) 109193. https://doi.org/10.1016/j.matdes.2020.109193.